A combined omics study on activated macrophages—enhanced role of STATs in apoptosis, immunity and lipid metabolism

Ashok Reddy Dinasarapu[1,†], Shakti Gupta[1,†], Mano Ram Maurya[1], Eoin Fahy[1], Jun Min[1], Manish Sud[2], Merril J. Gersten[1], Christopher K. Glass[3] and Shankar Subramaniam[1,2,3,4,*]

[1]Department of Bioengineering, [2]San Diego Super Computer Center, [3]Department of Cellular and Molecular Medicine and [4]Department of Chemistry and Biochemistry, University of California San Diego, CA 92093, USA

Associate Editor: Martin Bishop

ABSTRACT

Background: Macrophage activation by lipopolysaccharide and adenosine triphosphate (ATP) has been studied extensively because this model system mimics the physiological context of bacterial infection and subsequent inflammatory responses. Previous studies on macrophages elucidated the biological roles of caspase-1 in post-translational activation of interleukin-1β and interleukin-18 in inflammation and apoptosis. However, the results from these studies focused only on a small number of factors. To better understand the host response, we have performed a high-throughput study of Kdo2-lipid A (KLA)-primed macrophages stimulated with ATP.

Results: The study suggests that treating mouse bone marrow-derived macrophages with KLA and ATP produces 'synergistic' effects that are not seen with treatment of KLA or ATP alone. The synergistic regulation of genes related to immunity, apoptosis and lipid metabolism is observed in a time-dependent manner. The synergistic effects are produced by nuclear factor kappa-light-chain-enhancer of activated B cells (NF-kB) and activator protein (AP)-1 through regulation of their target cytokines. The synergistically regulated cytokines then activate signal transducer and activator of transcription (STAT) factors that result in enhanced immunity, apoptosis and lipid metabolism; STAT1 enhances immunity by promoting anti-microbial factors; and STAT3 contributes to downregulation of cell cycle and upregulation of apoptosis. STAT1 and STAT3 also regulate glycerolipid and eicosanoid metabolism, respectively. Further, western blot analysis for STAT1 and STAT3 showed that the changes in transcriptomic levels were consistent with their proteomic levels. In summary, this study shows the synergistic interaction between the toll-like receptor and purinergic receptor signaling during macrophage activation on bacterial infection.

Availability: Time-course data of transcriptomics and lipidomics can be queried or downloaded from http://www.lipidmaps.org.

Contact: shankar@ucsd.edu

Supplementary information: Supplementary data are available at *Bioinformatics* online.

Received on March 20, 2013; revised on July 22, 2013; accepted on August 8, 2013

1 INTRODUCTION

Lipopolysaccharide (LPS) is an endotoxin from bacterial cell wall that stimulates leukocytes via a *toll-like receptor* (TLR)-4 pathway (Peck *et al.*, 2004). Kdo2-lipid A (KLA) is an active component of LPS with an analogous response (Raetz *et al.*, 2006) in activating macrophages. The TLR-4 signaling pathway ultimately mediates the release of pro- and anti-inflammatory factors by activating mitogen-activated protein kinase cascade, nuclear factor kappa-light-chain-enhancer of activated B cells (NF-κB) and/or activator protein (AP)-1 (Maurya *et al.*, 2013; Raetz *et al.*, 2006; Rutledge *et al.*, 2012). In this study, we have primed macrophages with KLA before stimulation with ATP. KLA priming represents bacterial exposure, which elicits subsequent release of ATP in the extracellular space from inflamed, damaged or dying cells. ATP then acts via autocrine and paracrine signaling and is interpreted as a 'danger signal' by immune cells. These events induce the transcription of pro-inflammatory mediators through the transcription factors (TFs) NF-κB and AP1 (Junger, 2011). Interestingly, a model system of ATP stimulation of LPS-primed macrophages exhibited increased cell death compared with the macrophages treated with either ATP or LPS alone (Mehta *et al.*, 2001; Pfeiffer *et al.*, 2007). The increased apoptosis, caused by LPS and ATP treatment, was reduced with caspase-1 inhibitors but not with mitogen-activated protein kinase, protein kinase (PK)-C, or PK-A inhibitors (Mehta *et al.*, 2001; Pfeiffer *et al.*, 2007). In addition to LPS and ATP treatment, there have been a number of studies on LPS-primed macrophages stimulated by various ligands including air particles, lysophosphatidic acid, interferon (IFN)-γ, IL-4 and toxicants (El Chartouni and Rehli, 2010; Glaser *et al.*, 1993; Griffiths *et al.*, 1995; Gupta *et al.*, 2010; Imrich *et al.*, 1999; Le Feuvre *et al.*, 2002; Pelegrin *et al.*, 2008; Pestka and Zhou, 2006; Uehara *et al.*, 2002). Moreover, sequential activation of one or more TLR receptors by their respective ligands was studied in LPS-primed macrophages (De Nardo *et al.*, 2009; Ilievski and Hirsch, 2010). Most of these studies showed the importance of selected genes or cytokines in LPS-primed macrophages to mimic the biological context of bacterial infection and subsequent immune response.

In addition to the cytokine response, LPS-stimulated macrophages showed changes in lipids such as eicosanoids, sphingolipids, sterols, glycerolipids and glycerophospholipids (Chang *et al.*, 2001; Dennis *et al.*, 2010; Desanctis *et al.*, 1994; Drapier and Petit, 1986; Hauton and Evans, 2002; Knapp and English,

*To whom correspondence should be addressed.
†The authors wish it to be known that, in their opinion, the first two authors should be regarded as joint First Authors.

2000; MacKichan and DeFranco, 1999; Rovina *et al*., 2010; White *et al*., 1988). Each of these lipids has distinct roles in various physiological processes and diseases. For example, prostaglandins play important role in inflammation; sphingolipids regulate cell proliferation and apoptosis; and sterols play a central role in atherosclerosis (Wymann and Schneiter, 2008). The changes to each of the lipid categories, therefore, are important mediators in bacterial exposure. However, no previous macrophage study considered transcriptomic and lipidomic changes during KLA and ATP treatment in a time-dependent manner.

In this work, we have studied KLA-primed macrophages stimulated with ATP in high-throughput transcriptomics and metabolomics (lipidomics) experiments. The goal of the work was to analyze the lipidomic and transcriptomic changes. In particular, we performed enrichment analysis and TRANSFAC® (Wingender *et al*., 1996) mapping on differentially regulated genes and showed the distinct roles of STAT1 and STAT3 on apoptosis, immunity and lipid metabolism.

2 METHODS

2.1 Transcriptomic and lipidomic data

Transcriptomic and lipidomic data were generated in mouse bone marrow-derived macrophages (BMDM) over 7 time points, 0.25, 0.5, 1, 2, 4, 8 and 20 h, with three different stimulus conditions: 2 mM ATP (A), 100 ng/ml KLA (K) and KLA/ATP (KA) treatments by the Lipid Metabolites and Pathways Strategy (LIPID MAPS) consortium (Dennis *et al*., 2010; Subramaniam *et al*., 2011). To confirm the activation of macrophages, TNF-α was used as a marker (Guerra *et al*., 2003; Tonetti *et al*., 1995). For the KA group, treatment with K was performed 4 h before treatment with A; this was done to mimic the biological phenomenon of KLA activation preceding ATP release as a 'danger signal' from immune cells (Supplementary Fig. S1). For the transcriptomic data, two biological replicates were measured with dye swap using Agilent custom microarrays. The arrays contained 45 214 spots with 38 838 unique probes and 21 676 unique mouse genes. The data were normalized using the locally weighted scatterplot smoothing (Lowess) method (Yang *et al*., 2002). For lipidomic data, three biological replicate experiments were carried out using liquid chromatography and mass spectrometry techniques. The detailed protocols are described in LIPID MAPS Web site (http://www.lipidmaps.org/protocols/index.html).

2.2 Statistical analysis

2.2.1 Regulated list of probes and genes To identify significantly regulated probes, variance modeling-based *t*-test (implemented as Cyber-T) was used (Baldi and Long, 2001). Cyber-T uses a Bayesian estimate of the variance among the probe intensities. We applied Cyber-T in two different ways. In the *Case I* analysis, a paired *t*-test was used to find the differentially regulated probes between treatment and its control group (Fig. 1). In the *Case II* analysis, an unpaired *t*-test was used to identify the probes that are differentially regulated between single and combined treatment groups; specifically, KA data were used as the treatment group and K or A data as control group. For this analysis, the raw intensity values of K, A and KA data were used under the assumption that the (true) control intensity values are approximately same across the three conditions (see Section 2.2.2). We chose to use raw intensity values in the *Case II* analysis, instead of the fold changes with respect to controls, because variance of the data, used to calculate the *t*-scores, should be estimated locally among probes with similar raw intensity values. In both analyses, a gene was identified as significantly regulated if its associated *P*-value was ≤0.001. To analyze the differentially regulated probes,
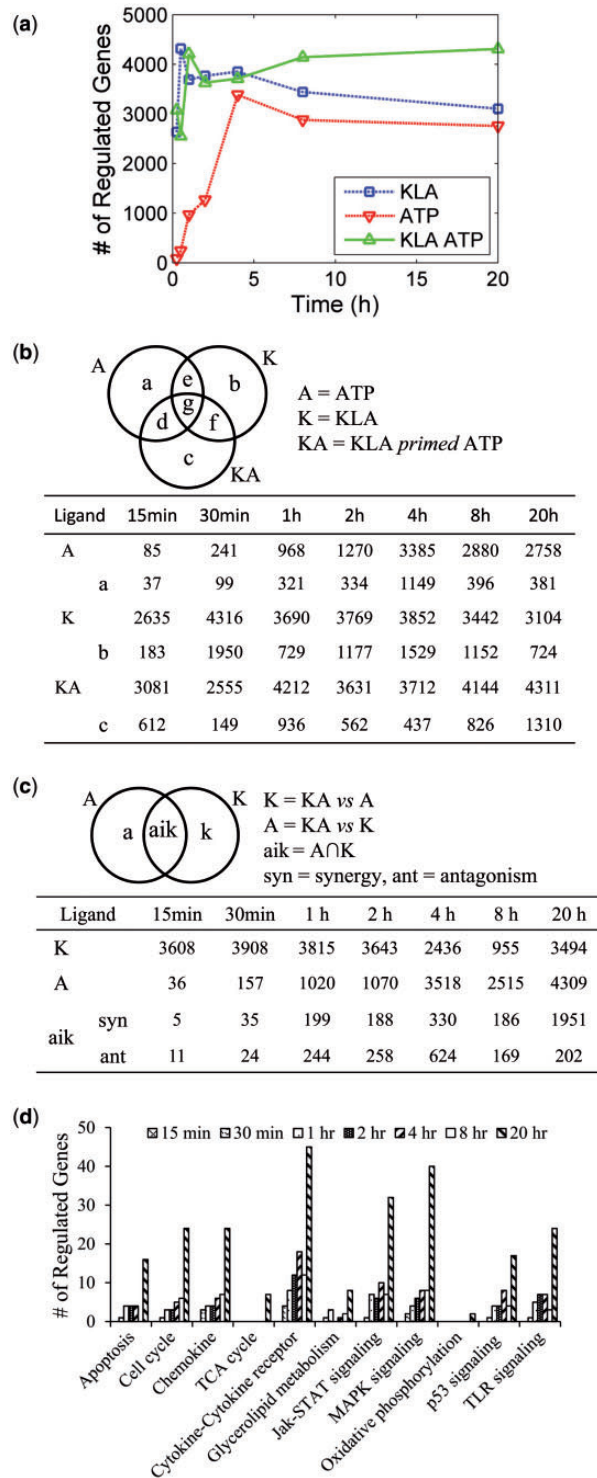

Fig. 1. Differentially regulated gene lists of ATP (A), KLA (K), and KLA/ATP (KA) groups at 7 time points. (**a**) Number of significantly regulated genes for three different treatment groups with respect to their controls, (**b**) Venn diagram of three different treatment groups with respect to their controls from *Case I* analysis, and (**c**) Venn diagram of the KA group versus the A or the K group from *Case II* analysis and (**d**) Number of *Case II* synergistic genes in enriched KEGG pathways by time point(s), *y*-axis represents number of regulated genes

we mapped them to their Entrez gene IDs and obtained the unique list of genes. Probes mapping to the same gene, but with opposite regulated expression, were removed from further analysis.

Generally, multiple testing correction methods (Dudoit and Laan, 2008) such as false discovery rate (FDR) and Bonferroni correction are used for refining *P*-values. However, we did not use either correction methods for the following reasons: Bonferroni correction was deemed too stringent, and FDR created a problem in identifying the list of regulated genes for early time points in A data. For example, FDR did not produce any significantly regulated gene for 15 or 30 min in the ATP treatment because of low number of differentially regulated genes at those time points.

2.2.2 Outlier detection One of the key assumptions in using an unpaired *t*-test for the treatment gene expression values in the *Case II* analysis is the stability of the (true) control expression values across the different ligand groups (K, A and KA). However, in some cases a probe's control value for one of the ligands was significantly different from the other two, causing the *t*-test results to be misleading. To address this issue, the Grubbs test for outliers (Grubbs, 1950) was used on the (true) control expression values to identify potential outliers. Probes were removed from statistical analysis if one of their control values was more extreme than either twice or half the mean of all three control values. The second test was necessary to ensure that the results from the Grubbs test did not overestimate the number of potential outliers because of the small sample size ($N = 3$). The condition for the Grubbs test is given below:

$$\frac{\displaystyle\max_{i=1,\ldots,N}|Y_i - \bar{Y}|}{s} > \frac{N-1}{\sqrt{N}}\sqrt{\frac{t^2_{\alpha/(2N), N-2}}{N-2+t^2_{\alpha/(2N), N-2}}}$$

The hypothesis of no outliers was rejected if the above condition is satisfied where $\bar{Y}$ is the sample mean, s is the standard deviation, N is the sample size and $t_{\alpha/(2N), N-2}$ is the critical value of *t*-distribution. We used a *P*-value threshold of 0.05. For further information, see Supplementary Table S1.

2.2.3 Functional enrichment analyses Enrichment analysis was performed to identify the significance of the changes in the differentially regulated genes based on different biological processes. Gene Ontology (Ashburner *et al.*, 2000) and Kyoto encyclopedia of genes and genomes pathways (Kanehisa and Goto, 2000) were used to identify overrepresented annotation groups by comparing a 'selected' list with a 'background'. A comprehensive gene list of the microarray was considered as a background. The hypergeometric distribution was used to find the exact probabilities to compute enrichment likelihoods (Hsiao *et al.*, 2005):

$$P(\geq s) = \sum_{i=s}^{b} \frac{\binom{b}{i}\binom{N-b}{k-i}}{\binom{N}{k}}$$

where *b* is the number of 'background' genes annotated with the term/pathway, *s* is the number of 'selected' genes annotated with the term/pathway, *N* is the total number of 'background' genes and *k* is the total number of 'selected' genes.

2.2.4 TF-target gene mapping TRANSFAC® Release 2010.4 data were used as the source for TF—target gene information. For each time point, the TFs in the differentially regulated list of genes were selected and mapped to their subset of target genes that were also differentially regulated at the same or a later time point. As there are 7 time points, there exist 21 iterations [n (n − 1)/2, where $n = 7$ time points]. The regulated network was created and visualized using GraphViz (www.graphviz.

org) and/or Cytoscape (www.cytoscape.org). Upregulated genes are colored red (or solid nodes) and downregulated genes are colored green (or dashed nodes); the time points 1, 2, 3, 4, 5, 6 and 7 represent 0.25, 0.5, 1, 2, 4, 8 and 20 h, respectively (Fig. 2).

2.2.5 Correlation/clustering of lipid profiles Pearson correlation is used to find the similarity between two time courses (Anderson, 1984; Egghe and Leydesdorff, 2009). For our data, we used a weighted correlation, in which the time points were weighted in proportion to the preceding time interval, because the measurements were taken at nonuniform time intervals (Dennis *et al.*, 2010). For example, the earlier time points had less weight because the measurements were taken more frequently in the beginning than at the end (Subramaniam *et al.*, 2011). Assuming a weight vector of $W = [w_1, w_2, w_3, w_4, w_5, w_6, w_7]$, the weighted mean, the weighted standard deviation, the weighted *z*-score and the correlation were computed as follows (where $n = 7$, the number of time points):

$$\text{Mean}: \bar{X}_w = \left(\sum_{i=1}^{n} w_i x_i\right) / \sum_{i=1}^{n} w_i; \quad \bar{Y}_w = \left(\sum_{i=1}^{n} w_i y_i\right) / \sum_{i=1}^{n} w_i$$

$$\text{Standard deviation}: \bar{\sigma}_{x,w} = \sqrt{\left(\sum_{i=1}^{n} w_i(x_i - \bar{X}_w)^2\right) / \sum_{i=1}^{n} w_i}$$

$$\text{Compute } \bar{\sigma}_{y,w}$$

$$z-\text{score}: X_{z,w} = \left(X - \bar{X}_w\right)/\bar{\sigma}_{x,w}; \quad Y_{z,w} = \left(Y - \bar{Y}_w\right)/\bar{\sigma}_{y,w}$$

$$\text{Correlation}: r_w = \left(\sum_{i=1}^{n} w_i(X_{z,w})_i(Y_{z,w})_i\right) / \sum_{i=1}^{n} w_i$$

The above equations were extended for two data matrices X and Y, with the rows representing different genes or lipids and the columns representing different time points. Correlation-based hierarchical clustering (Langfelder *et al.*, 2008) was used to lay out the variables (lipid concentrations or gene fold changes) in the data heat map. The data shown are the differences in treatment versus control values scaled by the maximum absolute value of each row. The statistics/bioinformatics toolbox of Matlab® (Mathworks, 1994) was used to perform hierarchical clustering with the customized correlation defined earlier in the text [parameters: linkage-method = average; cut-off criterion = distance (=1− *r*); cut-off = 0.40]. Different colors for the names of the lipids indicate the clusters (Fig. 3).

3 RESULTS

We used paired *t*-test between experiments and control (*Case I* analysis) and unpaired *t*-test between the three treatments (*Case II* analysis) to identify differentially regulated genes (see Section 2). The results from the paired *t*-test in the *Case I* analysis showed few significantly regulated genes in the A group at 15 min (0.25 h), with the number increasing from 15 min to 4 h and then decreasing (Fig. 1a and b). In the case of K and KA groups, 4 h priming with K before the first measurement affected many genes, so that the number of significantly regulated genes at 15 min was ~3000. In the K group, the number of significantly regulated genes peaked at 30 min (equivalent to 4 h 30 min after treatment with K) and decreased substantially after 30 min. In contrast, the KA group showed the number of regulated genes to remain high for most of the time points.

To identify the similarities and the differences across the different treatments, Venn diagrams were drawn for all the time points (Fig. 1b and Supplementary Table S2). The results suggested that there is a significant number of regulated genes
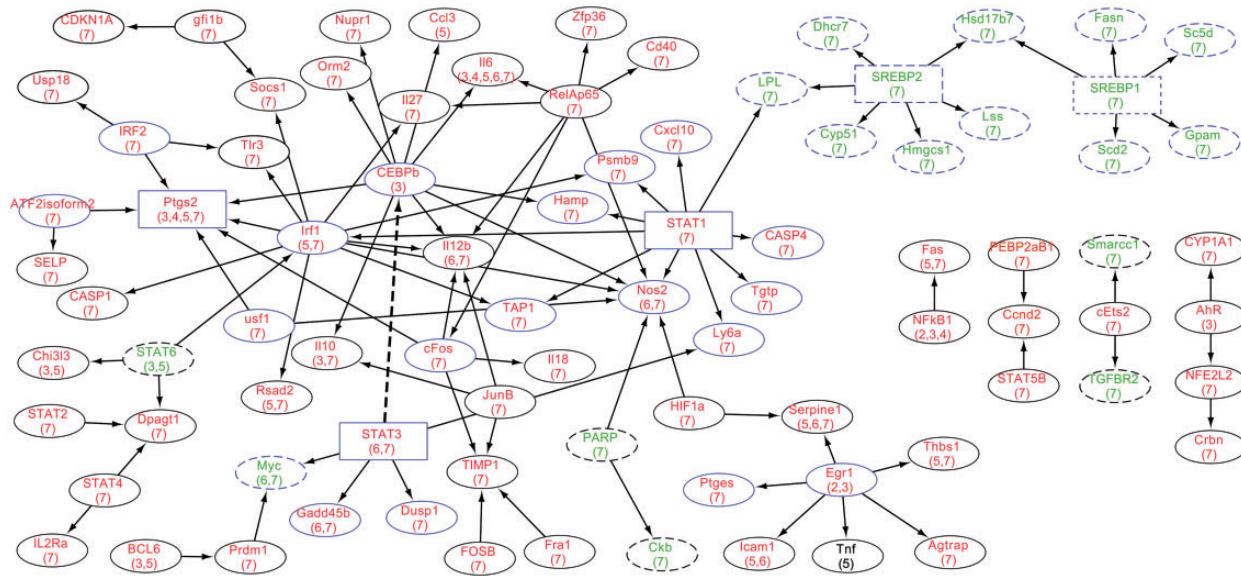
Fig. 2. Transcriptional regulatory network of Case II analysis spanning 7 time points (aik region in Fig. 1c). The TF to target interaction data was obtained from TRANSFAC. Edges between TFs and their targets were assigned when both were synergistically regulated, with the target regulated at the same or a later time point. The numbers 1, 2, 3, 4, 5, 6 and 7 represent 0.25, 0.5, 1, 2, 4, 8 and 20h, respectively. The red color (or solid nodes) indicates upregulation and the green color (or dashed nodes) indicates downregulation. Genes discussed in this manuscript are represented as rectangles. Dashed edge is added manually (see details in Section 4)

unique to the KA treatment (zone c in the Venn diagram), not regulated in either the K or the A treatment alone. However, *Case I* analysis has two problems. The first problem relates to false 'KA-unique' genes that showed up as differentially regulated genes in the KA treatment because of slight differences in *P*-values near the threshold. For example, a gene with a *P*-value just below the threshold in the KA treatment, but just above it in the K or A treatment, would, erroneously, be identified as unique to the KA treatment. The second problem relates to missed 'KA-unique' genes, genes differentially regulated in all three treatment groups, but significantly more regulated in the KA group than in the K or the A group as a result of synergistic effect. To circumvent these problems, the *Case II* analysis of the unpaired *t*-test between the treatment groups was adopted.

In the *Case II* analysis, two independent unpaired *t*-tests were performed: between KA and K groups, and between KA and A groups. The results from the first *t*-test produced the list of the genes that are differently regulated in the KA group compared with the K group. These genes were either affected by A or synergistically affected by KA (Fig. 1c, circle 'A'). Similarly, the genes from the second *t*-test were either affected by K or synergistically affected by KA (Fig. 1c, circle 'K'). The intersection between the two *t*-test results, then, produced the list of genes that are differently regulated in the KA group compared with both the K and the A groups (Fig. 1c, intersection 'aik'). Uniquely regulated genes in the KA group were categorized into synergistic and antagonistic subsets based on the direction and the magnitude of the regulation in the two comparisons. 'Synergistic regulation' is used here in a less restricted manner to include genes significantly regulated by KA as compared with K and A alone. This view includes but goes beyond the traditional definition of synergism (Chou, 2010); this approach

was taken to identify all the genes regulated by both K and A. A gene was considered to be synergistically regulated if its regulation in the KA group versus both the K and the A group was significantly higher or lower. For example, a gene that shows a 10-fold change in the KA group but only 5-fold changes in both the K and the A group was considered to be synergistically upregulated. Other possible cases of the synergistic effect are defined in Supplementary Figure S2. On the other hand, a gene was considered to be antagonistic if its regulation in the KA group was upregulated with respect to the K group but downregulated with respect to the A group, or vice versa.

Pathway enrichment for the *Case II* synergistic genes was done for all the time points to find the pathways that are synergistically affected by the KA treatment. Figure 1d shows the histogram of the number of regulated genes for all the time points in selected top enriched pathways. TFs from the *Case II* synergistic set of genes were also mapped to the subset of their target genes, which showed synergistic regulation at the same or future time points (Fig. 2). For *Case I*, TF-target genes mapping, see Supplementary Figure S3. The results of *Case II* analyses are presented here.

3.1 Signaling pathways

Pro- and anti-inflammatory cytokines: K and/or A signaling cascades include NF-κB and AP1 effector molecules in the activation of pro- and anti-inflammatory cytokines (Akira and Takeda, 2004; Tonetti *et al.*, 1995). In our data, K influenced AP1 via Jun, whereas A activated AP1 via both Jun and Fos. We found evidence of synergistic regulation of NF-κB and AP1 in the KA treatment. NF-κB was synergistically upregulated
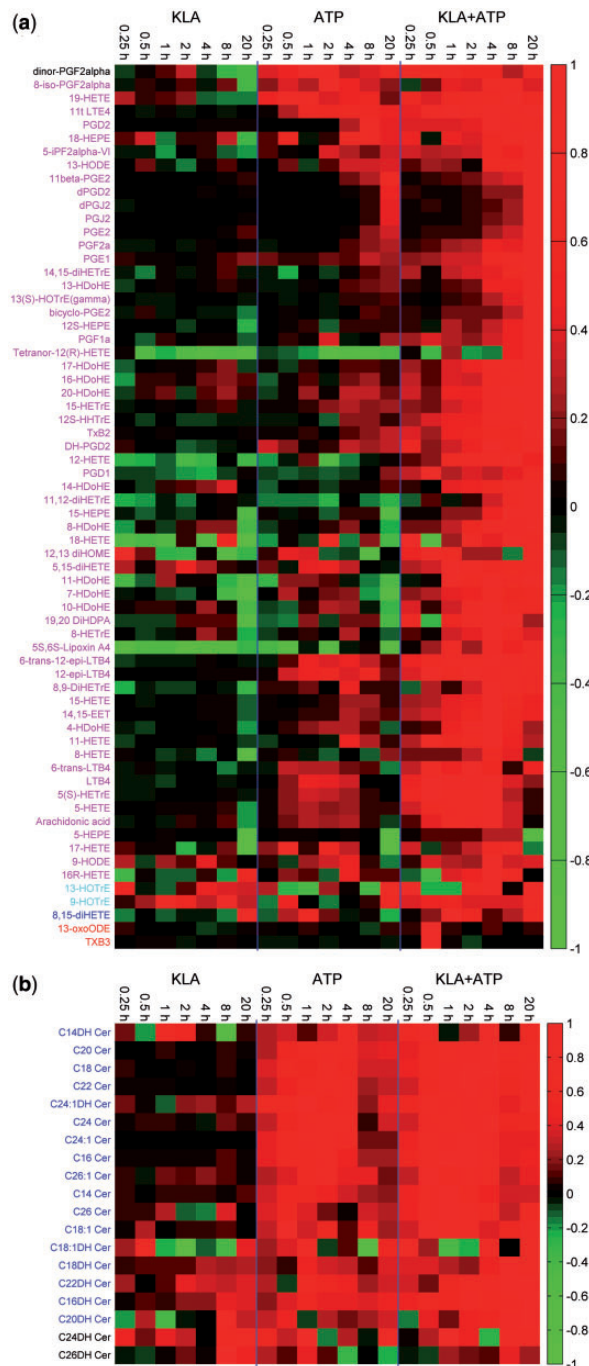
Fig. 3. Profiles of (**a**) eicosanoids and (**b**) sphingolipids. BMDM were treated with KLA and/or ATP. Heat map of lipid metabolite data based on time-weighted correlation-based clustering. The red color indicates upregulation and the green indicates downregulation (dinor-PGF2-alpha: 2,3-dinor-11b-PGF2α; dPGD2: 15-deoxy-delta-12,14-PGD2; dPGJ2: 15-deoxy-delta-12,14-PGJ2; DH-PGA2: 13,14-dihydro-15-keto-PGA2 and DH-PGD2: 13,14-dihydro-15-keto-PGD2)

starting from 1 h. ATF 1/2/3 and Junb showed statistically significant synergistic regulation at 20 h, although evidence of synergistic regulation was seen from 4 h onward. The synergistic activation of NF-κB and AP1 supported the synergistic effect

in TLR-4 signaling (Fig. 1d, Supplementary Fig. S4). The activated TLR-4 signaling promoted expression of pro- and anti-inflammatory cytokines, evidenced by enrichment of the cytokine–cytokine receptor interaction pathway from 30 min onward (Supplementary Table S3). Interleukins (ILs) are targets of TLR-4 signaling, and many of them showed, as expected, synergistic regulation in the KA treatment. For example, pro- and anti-inflammatory IL-6, IL-10 and IL-12 b were initially upregulated by CEBPβ, NF-κB and AP1 from 1 h onward (Fig. 2). TRANSFAC data mapping (Fig. 2) also shows that IL-27 was synergistically upregulated by NF-κB and Irf1, IL-12β by JunB and Fos and IL-18 by Fos.

JAK-STAT signaling pathway: Cytokines such as IL-6, IL-10, and IFN-β1 activate JAK-STAT signaling pathway via autocrine signaling (Murray, 2007). The pathway enrichment showed that JAK-STAT signaling was upregulated from 1 h onward (Supplementary Table S3). This is due to Jak2 and STATs, with the exception of STAT6, showing synergistic upregulation at 20 h. In particular, STAT3 was synergistically upregulated as early as 1 h, although statistical significance was not observed until 8 h. From Figure 2, TRANSFAC mapping shows that STAT3 synergistically upregulated Ly6a, which is known to promote phagocytosis by macrophages (Long *et al.*, 2011). Other members of the Ly6 complex were also synergistically upregulated in the KA treatment. Besides STAT3's involvement in phagocytosis, STAT1 has been shown to upregulate anti-microbial/viral factors such as Ly6a, Nos2, Hamp, Psmb9, TAP1 and Tgtp (Cramer and Klemsz, 1997; Lafuse *et al.*, 1995; Pagani *et al.*, 2011). Thus, STATs, particularly STAT1 and STAT3, that were synergistically upregulated in the KA treatment, are the key players in promoting phagocytic and anti-microbial functions of macrophages at later time points.

Cell cycle and apoptosis: Mapping of KA synergistic genes in the cell cycle pathway indicated that CycH and Myc were synergistically downregulated in KA (Supplementary Fig. S6). Myc has been shown to promote cell cycle progression by directly inducing CycD and sequestration of Kip1 (Amati *et al.*, 1998; Bouchard *et al.*, 1999). The synergistic upregulation of Bmip1 (an inhibitor of Myc) and Kip1 (an inhibitor of CycA) is consistent with the downregulation of Myc in the KA treatment. Known upstream inhibitors of cyclins (CycA/B/D/E), such as GSK3, Ink4d, Kip1/2, Cip1, GADD45b (a target of STAT3) and 14-3-3σ, were also synergistically upregulated. Thus, synergistic upregulation of cell cycle inhibitors and synergistic downregulation of cyclins accounted for the synergistic downregulation of the cell cycle. Pathway enrichment analysis also showed synergistic upregulation of apoptosis and p53 signaling pathways 1 h onward (Fig. 1d). The number of synergistically regulated genes in these pathways was initially low, but increased at 20 h indicating elevated cell death at later hours. This analysis observed synergistic upregulation of apoptotic genes such as caspase 1, 3, 4, 7, 8 and 12, as well as IL-1, FAS and Apaf1 (Le Feuvre *et al.*, 2002; Supplementary Fig. S5), and synergistic downregulation of anti-apoptotic genes (Bcl2) at 20 h. These results are also consistent with the observed reduction in DNA levels in KA experiments relative to control, K or A experiments (Supplementary Fig. S11).

3.2 Lipid metabolism

Eicosanoids: Eicosanoids, specifically prostaglandins (PGs), showed increased production in the KA treatment (Fig. 3a, Supplementary Fig. S7). The increase in PGs was in agreement with the observed synergistic upregulation of Ptgs2. TRANSFAC mapping (Fig. 2) shows that the synergistic upregulation of Ptgs2 was due to CEBPβ at early hours and Irf1, Irf2, Usf1 and AP1 at later hours. Further, Ptges and Alox12 also showed synergistic regulation at 20 h, consistent with the increased production of PGE2 and 12-HETE, respectively.

Sphingolipids: Increased concentrations of ceramide (Cer) and dihydroceramide were observed in the KA treatment (Fig. 3b and Supplementary Fig. S10). The enhanced synthesis (or accumulation) of Cers can be attributed to the synergistic upregulation of sphingolipid *de novo* synthesis enzyme, Sptlc2, in the KA treatment. Although sphingomyelin hydrolysis can also contribute to Cer levels via the upregulation of sphingomyelin synthase 2, reversible nature of this enzymatic reaction makes its contribution to the production of Cers less clear.

Sterols: The 3-hydroxy-3-methylglutaryl-coenzyme A (HMG-CoA) reductase was upregulated with respect to control in the KA treatment (*Case I* analysis), in agreement with the increased lanosterol and desmosterol in the KA treatment (Fig. 4). However, the concentrations of these sterols such as lanosterol and desmosterol were lower in the KA treatment than in the K treatment for most time points, suggesting ATP is influencing *de novo* synthesis of cholesterol and its precursors in KA treatment. These concentration profiles can be explained by the synergistic downregulation of several enzymes in the KA treatment involved in lanosterol and desmosterol synthesis: lanosterol synthase (Lss), lanosterol 14α demethylase (CYP51A1) and hydroxysteroid (17-beta) dehydrogenase 7 (HSD17B7). Furthermore, as seen in Figure 2 and Supplementary Figures S8 and S9, sterol regulatory element-binding protein1 (SREBP1) and SREBP2, known to regulate fatty acid and sterol biosynthesis enzymes including Lss, CYP51A1 and HSD17B7 (Rawson, 2003; Shimano, 2001),

are synergistically downregulated. Thus, synergistic downregulation of many genes in the sterol biosynthetic pathway contributes to reduced concentration profiles of sterols in the KA treatment compared with the profiles in the K treatment.

Glycerolipids: The profile of triglycerides (TGs), well-known glycerolipids, in Figure 4 shows an increased level in the KA treatment with respect to K and A treatments for most of the time points. These lipidomic data are explained by the synergistic upregulation of aldehyde dehydrogenase 1 family, member B1 (Aldh1b1), 1-acylglycerol-3-phosphate *O*-acyltransferase 4 (Agpat4), phosphatidic acid phosphatase type 2B (Ppap2b) and diacylglycerol *O*-acyltransferase 1 and 2 (Dgat1 & Dgat2), which are involved in the production of TGs from glycerols. Accumulation of TGs can also result from the reduced hydrolysis of TGs. In particular, lipoprotein lipase (LPL) is the rate-limiting enzyme for the hydrolysis (lipolysis) of TGs, and its expression has been shown to be suppressed by STAT1 and activated by SREBP2 at the transcriptional level (Hogan and Stephens, 2003; Wang and Eckel, 2009). Synergistic upregulation of STAT1 and downregulation of SREBP2 can lead to the synergistic downregulation of LPL in the KA treatment (Fig. 2), with an expected reduction in TG hydrolysis contributing to synergistic TGs accumulation (Fig. 4).

4 DISCUSSION

The activation of macrophages using KLA (or LPS) and/or ATP has been the subject of long-standing investigations because of their roles in inflammation, immunity and apoptosis. KLA treatment represents exposure of immune cells to bacteria; subsequently ATP is released from macrophages as a 'danger signal'. To globally study the macrophage role in inflammation and immunity, LIPID MAPS performed transcriptomic and lipidomic experiments on BMDM treated with KLA and/or ATP. Although this analysis is based on transcriptomic data, there is evidence of good correlation between gene and protein levels (Sabido *et al.*, 2012). We have validated the changes at the transcriptomic level for STAT1, STAT3 and SREBP2 with their proteomic levels using western blotting (see Supplementary Fig. S13). KLA (or LPS) treatment is known to release ATP into extracellular space. This concentration is generally much smaller than the concentration needed to sufficiently stimulate the macrophages *in vitro* and may produce a small amount of ATP-mediated autocrine signaling. In this analysis, such effects were ignored. Further, we identified differentially regulated genes and performed functional enrichment analysis for pathways and Gene Ontologies, and used TRANSFAC for TF to target gene mapping.

A time-dependent synergistic regulation of genes in both same and different signaling pathways and biological processes in the KA treatment was observed. In particular, both K and A influenced NF-κB and AP1 to produce synergistic regulations at the signaling level. At the transcriptional level, this synergistic effect was observed as early as 1 h. The synergistic activation of NF-κB and AP1 can also come from autocrine signaling through IL-1α or IL-1β. As a result, target chemokines and cytokines of NF-κB and AP1, such as IL-1, IL-6, IL-10 and Cxcl10, showed synergistic regulation for most of the time points. As IL-10 is known to inhibit the synthesis of several cytokines, including IFNα, IL-2
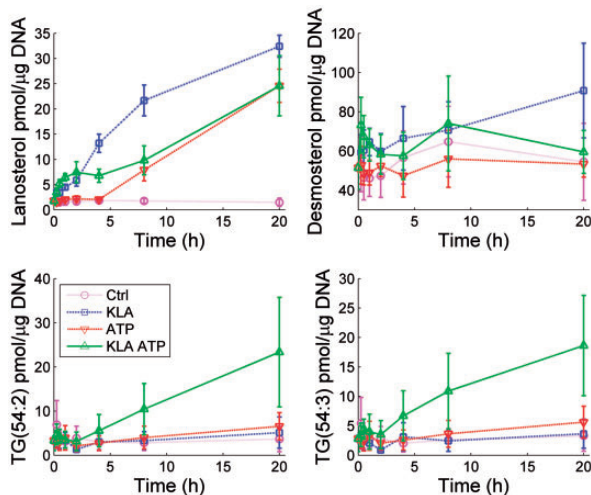

Fig. 4. Profiles of sterols and TGs. BMDM were treated with KLA and/ or ATP. The error bars shown for the experimental data represent the standard error of mean

and IL-3 (Isler *et al*., 1999), these cytokines did not show regulation in any of the treatments. TNF-α showed upregulation in all three cases individually, but in KA, upregulation was reduced because of A's inhibitory effect on K-primed macrophages and is consistent with previous results (Pinhal-Enfield *et al*., 2003) (shown with black, Fig. 2). The synergistic regulation of these cytokines and chemokines then induced a similar regulation of the cytokine–cytokine receptor pathway from 30 min onward and of the JAK-STAT pathway from 1 h onward. These time-dependent and synergistic regulations are consistent with previous studies. The enrichment of immediate/early genes and late response genes (Escoubet-Lozach *et al*., 2011) was seen at early and late hours, respectively, in our data (Supplementary Table S4). The synergistic activation and release of IL-1β, IL-18 and caspase1 in macrophages treated with LPS and/or ATP were observed in several previous studies (He *et al*., 2013; Kavita and Mizel, 1995). In addition, time-dependent regulation of TFs and their target genes was also observed. For Example, Ptgs2 was regulated by CEBPβ at early hours and Irf1, Irf2, Usf1 and AP1 at later hours. Similarly, IL-10 was regulated by CEBPβ at early hours and JunB at later hours. STAT1, SREBP1 and SREBP2 and their targets showed synergistic regulation at 20 h.

The changes at the transcriptional level are also reflected in the changes in the level of corresponding lipids (Supplementary Table S5). Eicosanoids, TGs and Cers had higher concentrations in the KA treatment than in the K or the A treatment and were consistent with the synergistic upregulation of Ptgs2, Sptlc2 and Aldh1b1, respectively. In case of the eicosanoids pathway, a good correlation has been observed between gene and protein levels in macrophages treated with KLA and KLA/ATP (Sabido *et al*., 2012). The accumulation of TGs was further because of reduced lipolysis and is consistent with a recent study in activated macrophages (Feingold *et al*., 2012). In addition, FAS, shown to be upregulated in the *de novo* synthesis of sphingolipid and the apoptosis pathway (Hannun and Obeid, 2008), was also upregulated in this study. Thus, the synergistic upregulation of FAS may contribute to increased sphingolipid metabolism and elevated expressions of apoptotic genes in the KA treatment. The synergistic downregulation of SREBP2 and its targets yielded decreased *de novo* synthesis of lanosterol and desmosterol in the KA treatment compared with that in the K treatment.

Pathway analysis and TF-target gene mapping suggest that STAT1 and STAT3 regulated apoptosis, immunity and lipid metabolism through many important genes directly or through a regulation cascade. Many STAT1 and STAT3 targets such as caspase-1, caspase-4, cMyc and GADD45b supported increased apoptosis and impaired cell cycle progression. Similarly, STAT1 and STAT3 synergistically regulated anti-microbial/viral genes such as Ly6a, Nos2, Hamp, Psmb9 and TAP1 (Cramer and Klemsz, 1997; Lafuse *et al*., 1995; Pagani *et al*., 2011). Further, many of the synergistically regulated genes that influence lipid metabolism were regulated by STATs. For example, a previous study showed that STAT3 activates CEBPβ (Cantwell *et al*., 1998); thus, STAT3 upregulated Ptgs2 through CEBPβ to increase arachidonic acid production in eicosanoid metabolism. STAT1 downregulated LPL and promoted accumulation of TGs because of reduced lipolysis.

Macrophages undergo either classical (M1) activation or alternative (M2) activation (Lawrence and Natoli, 2011). Macrophage polarization is regulated by STAT1 and STAT3 or STAT6. STAT1 regulates the M1 phenotype, whereas STAT3 or STAT6 regulates the M2 phenotype when macrophages are treated with different ligands (Sica and Mantovani, 2012). The synergistic upregulation of both STAT1 and STAT3 reflected a balance between M1 and M2 phenotypes. Downregulation of STAT-6 (the only synergistically downregulated STAT in KA) suggested STAT6 activation is not required for M2 phenotype in BMDM, a finding consistent with previous studies of macrophages (Csoka *et al*., 2012). Myc also controls a subset of M2-associated genes (Sica and Mantovani, 2012). The synergistic downregulation of Myc also suggested a predominant role of STAT3 in the M2 phenotype.

The synergistic activation of a gene was identified in our analysis when the fold change was statistically significant. However, a TF with fold change less than the statistical threshold may nevertheless be biologically effective and produce a significant transcriptional change in its target genes. For example, the synergistic upregulation of STAT3 was not statistically significant until 8 h but was observable as early as 1 h; the low-fold change of STAT3 at earlier time points, even if not statistically significant, could cause its target, CEBPβ, to be synergistically upregulated at 1 h (added as a dashed edge in Fig. 2).

In summary, our analysis suggests that the synergistic activation of macrophages in the KA treatment occurred through the activation NF-κB and AP1, which, in turn, activated cytokine release. The cytokine effector functions synergistically activated STATs, particularly STAT1 and STAT3, that lead to enhanced immunity, apoptosis and lipid metabolism. STAT1 played a prominent role in enhanced immunity by regulating anti-microbial factors. STAT3 was important in regulating cell cycle and enhancing apoptosis. In addition, STAT1 and STAT3 regulated TGs and eicosanoids metabolism, respectively. The observed synergistic regulations were time-dependent, encompassing multiple genes that span key pathways related to immunity, apoptosis and lipid metabolism and highlight the complexity of the combined TLR and purinergic receptor activation of macrophage activation during bacterial infection.

Conflict of Interest: none declared.

REFERENCES

Akira,S. and Takeda,K. (2004) Toll-like receptor signalling. *Nat. Rev. Immunol*., **4**, 499–511.

Amati,B. *et al*. (1998) Myc and the cell cycle. *Front. Biosci*., **3**, d250–d268.

Anderson,T.W. (1984) *An introduction to multivariate statistical analysis*. Wiley, New York.

Ashburner,M. *et al*. (2000) Gene ontology: tool for the unification of biology. The Gene Ontology Consortium. *Nat. Genet*., **25**, 25–29.

Baldi,P. and Long,A.D. (2001) A Bayesian framework for the analysis of microarray expression data: regularized t-test and statistical inferences of gene changes. *Bioinformatics*, **17**, 509–519.

Bouchard,C. *et al*. (1999) Direct induction of cyclin D2 by Myc contributes to cell cycle progression and sequestration of p27. *EMBO J*., **18**, 5321–5333.

Cantwell,C.A. *et al.* (1998) Interleukin-6-specific activation of the C/EBPdelta gene in hepatocytes is mediated by Stat3 and Sp1. *Mol. Cell. Biol.*, **18**, 2108–2117.

Chang,Y.H. *et al.* (2001) Effects of cannabinoids on LPS-stimulated inflammatory mediator release from macrophages: involvement of eicosanoids. *J. Cell. Biochem.*, **81**, 715–723.

Chou,T.C. (2010) Drug combination studies and their synergy quantification using the Chou-Talalay method. *Cancer Res.*, **70**, 440–446.

Cramer,L.A. and Klemsz,M.J. (1997) Altered kinetics of Tap-1 gene expression in macrophages following stimulation with both IFN-gamma and LPS. *Cell Immunol.*, **178**, 53–61.

Csoka,B. *et al.* (2012) Adenosine promotes alternative macrophage activation via A2A and A2B receptors. *FASEB J.*, **26**, 376–386.

De Nardo,D. *et al.* (2009) Signaling crosstalk during sequential TLR4 and TLR9 activation amplifies the inflammatory response of mouse macrophages. *J. Immunol.*, **183**, 8110–8118.

Dennis,E.A. *et al.* (2010) A mouse macrophage lipidome. *J. Biol. Chem.*, **285**, 39976–39985.

Desanctis,J.B. Effects of cannabinoids on LPS-stimulated inflammatory mediator release from macrophages: involvement of eicosanoids. (1994) Prostaglandins inhibit lipoprotein lipase gene expression in macrophages. *Immunology*, **81**, 605–610.

Drapier,J.C. and Petit,J.F. (1986) Development of antitumor activity in LPS-stimulated mouse granuloma macrophages. Regulation by eicosanoids. *Inflammation*, **10**, 195–204.

Dudoit,S. and Laan,M.J. (2008) *Multiple testing procedures with applications to genomics. Springer series in statistics.* Springer, New York; London.

Egghe,L. and Leydesdorff,L. (2009) The relation between Pearson's correlation coefficient r and Salton's cosine measure. *J. Am. Soc. Inf. Sci. Technol.*, **60**, 1027–1036.

El Chartouni,C. and Rehli,M. (2010) Comprehensive analysis of TLR4-induced transcriptional responses in interleukin 4-primed mouse macrophages. *Immunobiology*, **215**, 780–787.

Escoubet-Lozach,L. *et al.* (2011) Mechanisms establishing TLR4-responsive activation states of inflammatory response genes. *PLoS Genet.*, **7**, e1002401.

Feingold,K.R. *et al.* (2012) Mechanisms of triglyceride accumulation in activated macrophages. *J. Leukoc. Biol.*, **92**, 829–839.

Glaser,K.B. *et al.* (1993) Regulation of eicosanoid biosynthesis in the macrophage. Involvement of protein tyrosine phosphorylation and modulation by selective protein tyrosine kinase inhibitors. *Biochem. Pharmacol.*, **45**, 711–721.

Griffiths,R.J. *et al.* (1995) ATP induces the release of IL-1 from LPS-primed cells *in vivo*. *J. Immunol.*, **154**, 2821–2828.

Grubbs,F.E. (1950) Sample criteria for testing outlying observations. *Ann. Math. Stat.*, **21**, 27–58.

Guerra,A.N. *et al.* (2003) Purinergic receptor regulation of LPS-induced signaling and pathophysiology. *J. Endotoxin Res.*, **9**, 256–263.

Gupta,S. *et al.* (2010) Identification of crosstalk between phosphoprotein signaling pathways in RAW 264.7 macrophage cells. *PLoS Comput. Biol.*, **6**, e1000654.

Hannun,Y.A. and Obeid,L.M. (2008) Principles of bioactive lipid signalling: lessons from sphingolipids. *Nat. Rev. Mol. Cell. Biol.*, **9**, 139–150.

Hauton,D. and Evans,R.D. (2002) Utilisation of fatty acid and triacylglycerol by rat macrophages: the effect of endotoxin. *Cell Physiol. Biochem.*, **12**, 293–304.

He,Y. *et al.* (2013) TLR agonists stimulate Nlrp3-dependent IL-1beta production independently of the purinergic P2X7 receptor in dendritic cells and *in vivo*. *J. Immunol.*, **190**, 334–339.

Hogan,J.C. and Stephens,J.M. (2003) STAT 1 binds to the LPL promoter *in vitro*. *Biochem. Biophys. Res. Commun.*, **307**, 350–354.

Hsiao,A. *et al.* (2005) VAMPIRE microarray suite: a web-based platform for the interpretation of gene expression data. *Nucleic Acids Res.*, **33**, W627–W632.

Ilievski,V. and Hirsch,E. (2010) Synergy between viral and bacterial toll-like receptors leads to amplification of inflammatory responses and preterm labor in the mouse. *Biol. Reprod.*, **83**, 767–773.

Imrich,A. *et al.* (1999) Lipopolysaccharide priming amplifies lung macrophage tumor necrosis factor production in response to air particles. *Toxicol. Appl. Pharmacol.*, **159**, 117–124.

Isler,P. *et al.* (1999) Interleukin-12 production by human alveolar macrophages is controlled by the autocrine production of interleukin-10. *Am. J. Respir. Cell Mol. Biol.*, **20**, 270–278.

Junger,W.G. (2011) Immune cell regulation by autocrine purinergic signalling. *Nat. Rev. Immunol.*, **11**, 201–212.

Kanehisa,M. and Goto,S. (2000) KEGG: kyoto encyclopedia of genes and genomes. *Nucleic Acids Res.*, **28**, 27–30.

Kavita,U. and Mizel,S.B. (1995) Differential sensitivity of interleukin-1 alpha and -beta precursor proteins to cleavage by calpain, a calcium-dependent protease. *J. Biol. Chem.*, **270**, 27758–27765.

Knapp,K.M. and English,B.K. (2000) Ceramide-mediated stimulation of inducible nitric oxide synthase (iNOS) and tumor necrosis factor (TNF) accumulation in murine macrophages requires tyrosine kinase activity. *J. Leukoc. Biol.*, **67**, 735–741.

Lafuse,W.P. *et al.* (1995) Cloning and characterization of a novel cDNA that is IFN-gamma-induced in mouse peritoneal macrophages and encodes a putative GTP-binding protein. *J. Leukoc. Biol.*, **57**, 477–483.

Langfelder,P. *et al.* (2008) Defining clusters from a hierarchical cluster tree: the Dynamic Tree Cut package for R. *Bioinformatics*, **24**, 719–720.

Lawrence,T. and Natoli,G. (2011) Transcriptional regulation of macrophage polarization: enabling diversity with identity. *Nat. Rev. Immunol.*, **11**, 750–761.

Le Feuvre,R.A. *et al.* (2002) Priming of macrophages with lipopolysaccharide potentiates P2X7-mediated cell death via a caspase-1-dependent mechanism, independently of cytokine production. *J. Biol. Chem.*, **277**, 3210–3218.

Long,K.K. *et al.* (2011) Sca-1 influences the innate immune response during skeletal muscle regeneration. *Am. J. Physiol. Cell. Physiol.*, **300**, C287–C294.

MacKichan,M.L. and DeFranco,A.L. (1999) Role of ceramide in lipopolysaccharide (LPS)-induced signaling. LPS increases ceramide rather than acting as a structural homolog. *J. Biol. Chem.*, **274**, 1767–1775.

Mathworks (1994) The Mathworks, Inc.© 1994–2009. Natick, MA.

Maurya,M.R. *et al.* (2013) Analysis of inflammatory and lipid metabolic networks across RAW264.7 and thioglycolate-elicited macrophages. *J. Lipid Res.*, **54**, 2525–2542 .

Mehta,V.B. *et al.* (2001) ATP-stimulated release of interleukin (IL)-1beta and IL-18 requires priming by lipopolysaccharide and is independent of caspase-1 cleavage. *J. Biol. Chem.*, **276**, 3820–3826.

Murray,P.J. (2007) The JAK-STAT signaling pathway: input and output integration. *J. Immunol.*, **178**, 2623–2629.

Pagani,A. *et al.* (2011) Low hepcidin accounts for the proinflammatory status associated with iron deficiency. *Blood*, **118**, 736–746.

Peck,O.M. *et al.* (2004) Differential regulation of cytokine and chemokine production in lipopolysaccharide-induced tolerance and priming. *Cytokine*, **26**, 202–208.

Pelegrin,P. *et al.* (2008) P2X7 receptor differentially couples to distinct release pathways for IL-1beta in mouse macrophage. *J. Immunol.*, **180**, 7147–7157.

Pestka,J. and Zhou,H.R. (2006) Toll-like receptor priming sensitizes macrophages to proinflammatory cytokine gene induction by deoxynivalenol and other toxicants. *Toxicol. Sci.*, **92**, 445–455.

Pfeiffer,Z.A. *et al.* (2007) Nucleotide receptor signaling in murine macrophages is linked to reactive oxygen species generation. *Free Radic. Biol. Med.*, **42**, 1506–1516.

Pinhal-Enfield,G. *et al.* (2003) An angiogenic switch in macrophages involving synergy between toll-like receptors 2, 4, 7, and 9 and adenosine A(2A) receptors. *Am. J. Pathol.*, **163**, 711–721.

Raetz,C.R. *et al.* (2006) Kdo2-Lipid A of *Escherichia coli*, a defined endotoxin that activates macrophages via TLR-4. *J. Lipid Res.*, **47**, 1097–1111.

Rawson,R.B. (2003) The SREBP pathway—insights from Insigs and insects. *Nat. Rev. Mol. Cell. Biol.*, **4**, 631–640.

Rovina,P. *et al.* (2010) Modulation of ceramide metabolism in mouse primary macrophages. *Biochem. Biophys. Res. Commun.*, **399**, 150–154.

Rutledge,H.R. *et al.* (2012) Gene expression profiles of RAW264.7 macrophages stimulated with preparations of LPS differing in isolation and purity. *Innate Immun.*, **18**, 80–88.

Sabido,E. *et al.* (2012) Targeted proteomics of the eicosanoid biosynthetic pathway completes an integrated genomics-proteomics-metabolomics picture of cellular metabolism. *Mol. Cell. Proteomics*, **11**, M111.014746.

Shimano,H. (2001) Sterol regulatory element-binding proteins (SREBPs): transcriptional regulators of lipid synthetic genes. *Prog. Lipid Res.*, **40**, 439–452.

Sica,A. and Mantovani,A. (2012) Macrophage plasticity and polarization: *in vivo* veritas. *J. Clin. Invest.*, **122**, 787–795.

Subramaniam,S. *et al.* (2011) Bioinformatics and systems biology of the lipidome. *Chem. Rev.*, **111**, 6452–6490.

Tonetti,M. *et al.* (1995) Extracellular ATP enhances mRNA levels of nitric oxide synthase and TNF-alpha in lipopolysaccharide-treated RAW 264.7 murine macrophages. *Biochem. Biophys. Res. Commun.*, **214**, 125–130.

Uehara,A. *et al.* (2002) Priming of human oral epithelial cells by interferon-gamma to secrete cytokines in response to lipopolysaccharides, lipoteichoic acids and peptidoglycans. *J. Med. Microbiol.*, **51**, 626–634.

Wang,H. and Eckel,R.H. (2009) Lipoprotein lipase: from gene to obesity. *Am. J. Physiol. Endocrinol. Metab.*, **297**, E271–E288.

White,J.R. *et al.* (1988) Bacterial lipopolysaccharide reduces macrophage lipoprotein lipase levels: an effect that is independent of tumor necrosis factor. *J. Lipid Res.*, **29**, 1379–1385.

Wingender,E. *et al.* (1996) TRANSFAC: a database on transcription factors and their DNA binding sites. *Nucleic Acids Res.*, **24**, 238–241.

Wymann,M.P. and Schneiter,R. (2008) Lipid signalling in disease. *Nat. Rev. Mol. Cell. Biol.*, **9**, 162–176.

Yang,Y.H. *et al.* (2002) Normalization for cDNA microarray data: a robust composite method addressing single and multiple slide systematic variation. *Nucleic Acids Res.*, **30**, e15.